INT. J. REMOTE SENSING, 1995, VOL. 16, NO. 13, 2341–2356

Microwave radiometry of the atmosphere: an experiment from a sea-based platform during ERS-1 altimeter calibration

P. CIOTTI†, P. BASILI‡, G. D'AURIA, F. S. MARZANO and N. PIERDICCA

Department of Ingegneria Elettronica, University of Rome 'La Sapienza', via Eudossiana 18, 00184 Rome, Italy

(Received 5 August 1993; in final form 20 February 1995)

Abstract. A steerable dual-channel microwave radiometer was installed on top of an oceanographic tower off shore from the Venice lagoon (Italy) during the calibration experiment of the ERS-1 radar altimeter organized by the European Space Agency. Measurements of atmospheric brightness temperature were carried out over more than two months in the summer 1991. The main objective of the experiment was to obtain the tropospheric electromagnetic excess path length (ΔH) required for the correction of the radar altimeter on board the satellite. The instrument calibration and the parameter retrieval algorithms were the main problems to be addressed. The retrieval of other meterological parameters, namely the precipitable water vapour (V) and the integrated cloud liquid (L), was also assessed. An accuracy (r.m.s.) of about 0·8 cm in ΔH, 0·1 cm in V and 0·04 mm in L is expected, resulting in a significant improvement when compared to those available from conventional meteorological data.

1. Introduction

During the five-month commissioning phase after the launch of the European Remote-Sensing Satellite (ERS-1) in July 1991, a radiometric experiment was carried out for the calibration of the radar altimeter data (Duchossois 1991, Francis 1993). Indeed from the time delay measured by a radar altimeter it is possible to obtain the range measurement only if the phase velocity along the atmospheric path is known. The correction to be given to the range calculated in free space is called the electromagnetic excess path length which is given by the integrated value of the atmospheric refractivity along the path. The planned experiment was limited to the tropospheric correction expressed in terms of integrated values of pressure, temperature, water vapour and cloud liquid densities. The determination of the above atmospheric parameters can be obtained either by conventional meteorological instruments or by a dual channel microwave radiometer (Goldhirsch and Rowland 1982). In the first case we can use climatological values from historical meteorological data sets, or surface values of meteorological data, or data from radiosounding balloons; however, the accuracy would be poor for different reasons. Historical meteorological data are not always available along satellite tracks and they average too large extents of atmospheric conditions. Surface data can only be used when we

†P. Ciotti is now with the Department of Ingegneria Elettrica, University of L'Aquila, Poggio di Roio, 67040 L'Aquila, Italy.

‡P. Basili is now with the Institute of Elettronica, University of Perugia, Santa Lucia Canetola, 06143 Perugia, Italy

0143–1161/95 $10.00

can trust an accurate model of the troposphere for finding the vertical profiles of atmospheric parameters. Radiosounding data require time for their acquisition and they are available in a few meteorological stations and only a few times a day. It was thought therefore that microwave radiometry could give better results, although the other possibilities were also explored for comparison. In particular, *ad hoc* radiosounding balloon launches were also performed from the site chosen for the experiment, encountering however some practical difficulties.

The site which had been chosen for the experiment was exactly under the trajectory of the satellite on an oceanographic tower located in the North Adriatic Sea at some distance from the coast, thus avoiding local influence. In the framework of the European Space Agency (ESA) calibration experiment, a mobile laser station was located inland for providing an accurate satellite position, and tide gauges at the tower gave measurements of the sea level. The satellite and tower positions were connected to the same reference system by a network of Global Positioning System (GPS) receivers.

The opportunity to use a dual channel microwave radiometer for about three months in such a particular environment made it possible to experience other possibilities of retrievals and practical operative procedures beyond the scope of tropospheric corrections. In particular, it has been possible to get data on precipitable water vapour and cloud liquid. Both such parameters have useful applications in climatology, meteorology and weather forecasting (Westwater 1978). Furthermore, for operative difficulties during the experiment, specific routine procedures of measurements have been adopted. The radiometer calibration during the experiment has represented one of the major problems since difficulties in the equipment installation, the modification of the antenna system and the particular conditions during the measurements warned us not to trust entirely previous laboratory tests.

In this paper, after a short review of the theoretical background of microwave radiometry and a description of the experiment, the approach used for the instrument calibration is given and an analysis of the sources of errors is presented. The approach is based on the use of a blackbody at a given temperature, which entirely covers the radiometer antennas, and periodic observations of the radiation scenery of the atmosphere at different elevation angles (tipping curves). The method for retrieving the integrated atmospheric parameters is also illustrated. This makes use of a multiple regression technique in which the regressor variables are the atmospheric opacities computed from brightness temperatures measured in two microwave channels and surface meteorological parameters. The regression coefficients are found by making use of historical meteorological data stratified with respect to season and clear and cloudy atmospheric conditions. Results of excess path length corrections, precipitable water vapour and cloud liquid values are given and comparisons with conventional methods of estimation are also discussed.

2. Theoretical background

The altitude measurements of a satellite-borne radar altimeter are affected by the time delay due to the troposphere. For a vertical path the radar altimeter observes an excess path length equal to:

$$\Delta H = 10^{-6} \int_0^H N(z)\, dz \tag{1}$$

where $N(z)$ is the refractivity (function of the height z) and the integration extends from the surface of the Earth to the maximum altitude H at which the atmosphere

affects the radar altimeter signal. The corrections can be made very accurately only if the value of the atmospheric parameters and thus the refractivity $N(z)$ are known along the whole path.

In the troposphere, the refractivity can be separated into a dry component (N_d) and a wet component (N_w). In addition, the wet term should be also expressed as the sum of two contributions, due to water vapour and cloud liquid (N_v and N_1, respectively), so that the corresponding excess path lengths become:

$$\begin{aligned}\Delta H &= 10^{-6}\left(\int_0^H N_d(z)\,dz + \int_0^H N_v(z)\,dz + \int_0^H N_1(z)\,dz\right)\\ &= \Delta H_d + \Delta H_v + \Delta H_1 = \Delta H_d + \Delta H_w\end{aligned} \tag{2}$$

The tropospheric effects produce an excess path length in the order of 250 cm, predominantly due to the dry component; however the wet tropospheric correction, in the order of 10–30 cm, exhibits large variability due to the water vapour content changes.

In the absence of cloud liquid, the refractivity can be calculated from the following approximate formula (Bean and Dutton 1968):

$$N = 77{\cdot}6(P/T) + 3{\cdot}73\ 10^5\ (e/T^2) \tag{3}$$

where P is the total atmospheric pressure (mbar), e the partial pressure of water vapour (mbar) and T the atmospheric temperature (K). Correspondingly, the excess path length results by integrating (3):

$$\Delta H_d + \Delta H_v = 77{\cdot}6\ 10^{-6}\int_0^H P/T\,dz + 3{\cdot}73\ 10^{-1}\int_0^H e/T^2\,dz \tag{4}$$

The computation of $\Delta H_d + \Delta H_v$ can be carried out in a straightforward way from radiosounding data, if available. On the contrary, the cloud liquid contribution ΔH_1 requires the assumption of a cloud model, for quantifying the amount of liquid in the cloud on the basis of the available information (Decker *et al.* 1978, Slobin 1982). If radiosounding data are not available, ΔH can also be estimated by using surface measurements of atmospheric parameters and a suitable model of the atmosphere (Saastamoinen 1972). In this case the excess path length (in centimetres) becomes:

$$\Delta H_d = (2{\cdot}277\ 10^{-1} - 1{\cdot}11\ 10^{-3}\cos\phi)\,P_s \tag{5}$$

$$\Delta H_v = 2{\cdot}277\ 10^{-1}(0{\cdot}05 + 1255/T_s)\,e_s \tag{6}$$

where P_s (mbar) is the atmospheric pressure at the surface, ϕ is the latitude, e_s (mbar) and T_s (K) are, respectively, the water vapour partial pressure and the atmospheric temperature measured at the surface.

Since the actual profiles of pressure and temperature can be predicted fairly well from P_s and T_s, the dry term can be estimated fairly precisely from surface measurements. This is not so for the wet term, as the high variability and non-uniform mixing of the water vapour with the dry air makes it very difficult to predict the vertical distribution of water vapour from a surface measurement of humidity. Moreover, in (6) the cloud liquid contribution to the wet term is not taken into account.

Alternatively, ΔH_w can be inferred from microwave radiometric observations of brightness temperatures. At the microwave band, for an atmosphere in local

thermodynamic equilibrium, in the absence of precipitating clouds and neglecting the small contribution of ice, the radiative transfer equation leads to the following expression for the brightness temperature T_B apparent to a zenith-viewing microwave radiometer (Ulaby *et al.* 1981):

$$T_B = T_{BG} \exp(-\tau(0,\infty)) + \int_0^\infty k_a(z) T(z) \exp(-\tau(0,z))\, dz \tag{7}$$

where T_{BG} is the cosmic background temperature (2·75 K), $\tau(0,\infty)$ is the atmospheric opacity thereafter indicated with τ, $k_a(z)$ is the atmospheric absorption coefficient (m^{-1}), $T(z)$ is the physical temperature of the medium (K) and $\tau(0,z)$ is the optical depth:

$$\tau(0,z) = \int_0^z k_a(z')\, dz' \tag{8}$$

By making use of the definition of the mean radiating temperature T_{mr}, (7) can be simplified and the atmospheric opacity derived from it (Wu 1979):

$$\tau = \tau(0,\infty) = \ln\left[\frac{(T_{mr} - T_{BG})}{(T_{mr} - T_B)}\right] \tag{9}$$

The opacity accounts for the spectral absorption produced by oxygen, water vapour and cloud liquid. Therefore, the atmospheric opacity τ can be separated into a dry component τ_d, a water vapour component τ_v and a cloud liquid component τ_1, which are all frequency dependent. Under suitable hypothesis, τ_v and τ_1 can also be assumed proportional to, respectively, the precipitable water vapour V and integrated cloud liquid L (Westwater 1978):

$$\tau(f) = \tau_d(f) + \tau_v(f) + \tau_1(f) = \tau_d(f) + K_v(f)V + K_1(f)L \tag{10}$$

where f is the frequency, $K_v(f)$ and $K_1(f)$ are averaged mass absorption coefficients for vapour and liquid.

If we measure the atmospheric brightness temperature at two frequencies, the first one (f_1) on the shoulder of the 22·2 GHz water vapour absorption band (e.g. 20·6 GHz) and the other (f_2) within a window band sensitive to cloud liquid (e.g. 36·0 GHz), we can write (10) twice for the selected frequencies and solve for V and L that become therefore linearly related to the atmospheric opacities $\tau(f_1)$ and $\tau(f_2)$ estimated by using a dual-channel microwave radiometer (Westwater 1978). Furthermore, since the water vapour contribution ΔH_v is approximately linearly related to the atmospheric precipitable water vapour V (Goldfinger 1980) and so is the cloud liquid term ΔH_1 with L (Resch 1984), it turns out that the wet contribution ΔH_w to the excess path length can also be obtained from a linear combination of $\tau(f_1)$ and $\tau(f_2)$.

3. Description of the experiment

The estimation of the ERS-1 radar altimeter excess path length at the frequency of 13·8 GHz has been performed by a dual-channel microwave radiometer, installed on the C.N.R./I.S.D.G.M. *Acqua Alta* oceanographic tower, 13 m high above the sea level. The tower, fixed on the sea bottom, is located in the Northern Adriatic Sea, at about 15 km from the Venice lagoon (Italy). Measurements were carried out from the beginning of August to mid-October 1991 in accordance with the satellite passes

during the ERS-1 commissioning phase. The radiometer which was utilized for the experiment was developed by the SMA company (Florence, Italy). It was able to operate at the frequencies of 20·6 GHz and 36·0 GHz as a total power radiometer, as well as in Dicke mode or in AGC mode, using two reference sources (Ulaby *et al.* 1981). The radiometer antennas (two horn lens antennas) had a 3 dB beamwidth of about 4·5 degrees, approximately equal for the two channels, and side lobe levels better than −25 dB. The instrument was protected from environmental damages in an aluminium enclosure, mounted on a steerable base which allowed scanning both in azimuth and elevation. During the campaign, the AGC mode of operation was selected since it provided a better instrument stability, although to the detriment of its radiometric resolution. An integration time of one second was chosen, leading to a radiometric resolution of about 0·5 K. Figure 1 represents a picture of the instrument installed on top of the oceanographic platform.

The experimental site was equipped with conventional meteorological and oceanographic sensors. Pressure, relative humidity and air temperature were regularly measured during each radiometer data acquisition. A few balloon launches were also carried out from the tower for radiosounding the atmosphere, but only two were successful. In the absence of stations provided with radiosoundings near the coast, for a systematic comparison we had to refer to radiosoundings carried out at Udine, inland from Venice, at about 100 km from the tower, and at Brindisi along the Adriatic coast but about 700 km south-east of Venice. Figure 2 depicts the platform location, the ERS-1 ground track during the commissioning phase and the location of the Udine and Brindisi stations.

Brightness temperatures at zenith were measured regularly every three days, from afternoon till about midnight, when the ERS-1 was passing over the tower. Frequent observations of the sky scenery (zenithal angles from 0 to 65 degrees) were also performed during the campaign, mainly for calibration purposes.

4. Radiometer calibration

The relationship between the instrument output voltage V_0 and the brightness temperature of the atmosphere T_B had to be measured accurately. Moreover, the peculiarity of the environmental conditions during the experiment required the monitoring of the instrument performance without using adequate laboratory equipment. In order to do that, we had to rely on the following measurements: (*a*) tipping curve measurements performed routinely during the campaign; (*b*) measurement of the radiation of a blackbody box at about ambient temperature.

If the instrument operates within a limited range of brightness temperatures, the calibration curve is linear and two coefficients, gain G and bias B, can be defined for each channel, so that:

$$V_0 = GT_B + B \tag{11}$$

The tipping curve procedure is commonly used for evaluating the instrumental bias changes but, considering the linear relation (11) applicable, it could in principle furnish also gain and opacity. In fact, in the assumption of a horizontally homogeneous atmosphere, the brightness temperature as a function of the zenithal angle θ can be expressed by the following formula:

$$T_B(\theta) = T_{BG} \exp(-\tau m) + T_{mr}(\theta)(1\text{-}\exp(-\tau m)) \tag{12}$$

where m is the air mass equal to sec θ. By inserting (11) in (12), we get:

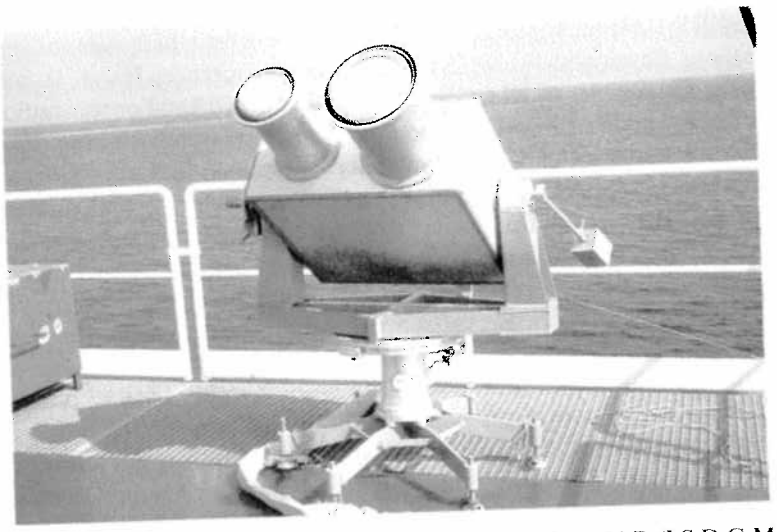

Figure 1. A picture of the radiometer installed on top of the C.N.R./I.S.D.G.M. oceanographic tower during the calibration of the ERS-1 radar altimeter. The radio frequency units of the 20·6 and 36·0 GHz channels are enclosed within a waterproof aluminium box mounted on a steerable base. The two horn antennas are protected from the marine environment by aluminium cylinders. The instrument control unit and the acquisition subsystem are installed elsewhere under the platform roof.

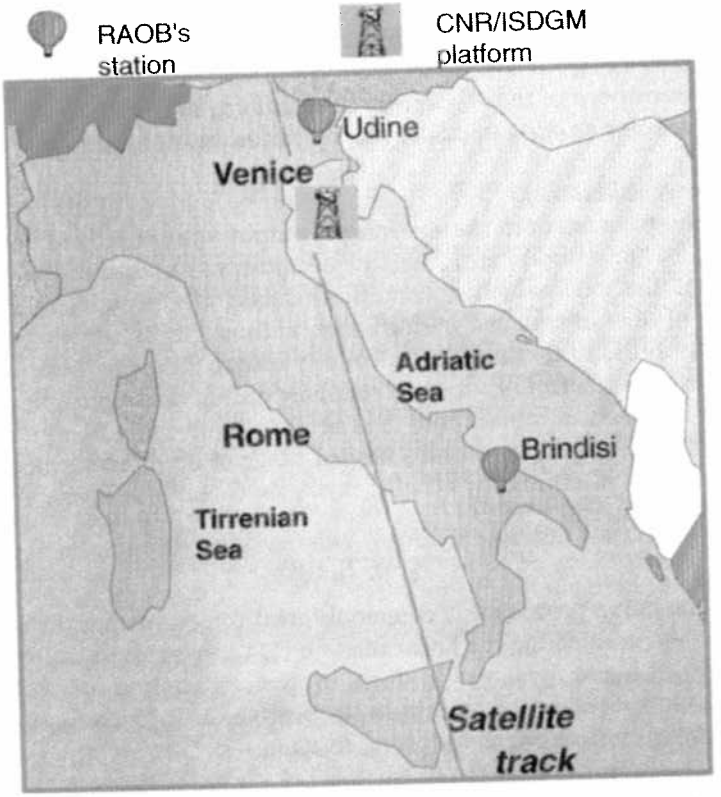

Figure 2. A schematic geographical map showing the location of the C.N.R./I.S.D.G.M. oceanographic tower (near Venice), the ERS-1 ground track during the commissioning phase and the position of the meteorological stations of Udine and Brindisi, whose radiosounding data have been used in this work.

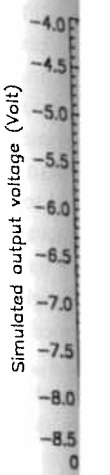

Figure 3. A simulate
20·5 GHz chan
The thick line
output voltage
resulting from

where $A = G T_{mr} + B$

Examining (13)
masses could solve
measure we want.
finding G and B. H
the curve of (13)
considering the lim
Starting from the
only $\theta = 65°$ ($m = 2$
antennas and poss
illustrated in figure
practically coincid
dependence of the

In addition, th
non-predictable an
atmospheric horiz
measurements, po
systematic errors r
width and sidelobe
differ from $T_B(\theta)$
coming directly fr
the antenna direc
negligible. A diffe
the radiometer wh

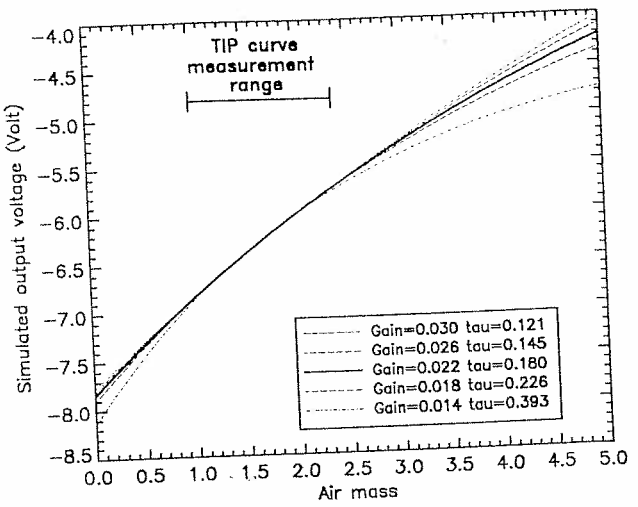

Figure 3. A simulated example showing the nature of the instability of the solution for the 20·5 GHz channel, when estimating G, B and τ by using a limited range of air masses. The thick line ($G=0{\cdot}022\,\mathrm{V\,m^{-1}}$, $B=7{\cdot}96\,\mathrm{V}$, $\tau=0{\cdot}18$) shows a simulated curve of output voltage as a function of air masses. It can be easily confused with curves resulting from different pairs of G and τ without appreciable variations of B.

$$V_0 = A + F\exp(-\tau m) \tag{13}$$

where $A = G\,T_{mr} + B$ and $F = G(T_{mr} - T_{BG})$.

Examining (13), we understand that radiometric measurements at several air masses could solve the problem of finding G, B and, at the same time, τ which is the measure we want. That is, we could obtain the opacity τ without the bother of finding G and B. However, a best fitting procedure to match experimental values to the curve of (13) would show a significant instability when finding A, F and τ, considering the limited extent of air masses which can be experimentally explored. Starting from the zenith ($m=1$), it was possible to extend the zenithal angle up to only $\theta=65°$ ($m=2{\cdot}37$). This limitation was due to the actual beamwidth of the antennas and possible obstacles in the surroundings. From a simulation analysis, illustrated in figure 3, it appears that diverse sets of G, B and τ give place to curves practically coincident in the considered air mass extent, thus confirming the weak dependence of the measured part of the tipping curve on variations of G, B and τ.

In addition, the exhibited instability of the solution must be confronted with non-predictable and systematic errors. The first ones include non-homogeneity in the atmospheric horizontal structure, time variability of the atmosphere during the measurements, pointing angle errors, instrumental noise and so on. Furthermore, systematic errors may derive from many causes. The effect of the antenna main lobe width and sidelobes should be taken into account, since the antenna temperature can differ from $T_B(\theta)$ because of the antenna convolution process and the radiation coming directly from the Earth's surface. However, a simulation has shown that, if the antenna directivity is sufficiently high and the angle θ is limited, this effect is negligible. A difference of less than 0·3–0·4 K has resulted for the antennas used in the radiometer when measuring up to a zenithal angle of 65°.

The value of the mean radiative temperature $T_{mr}(\theta)$ has been estimated as a linear combination of surface meteorological data. The coefficients have been calculated by a regression analysis based on four years of meteorological observations (Basili *et al.* 1994). The estimate of $T_{mr}(0)$ has shown an r.m.s. accuracy of about 3·5 K and the variation of T_{mr} with θ has been found negligible for the purpose of radiometer calibration. The effect of ray bending at pointing angles other than zenith has also been found negligible when the maximum zenithal angle is limited to 65° and so has been the correction of instrument non-linearity for the tipping curve measurements.

In order to improve the stability of the required solution, we have modified the best fitting procedure based on (13) for M values of zenithal angles by adding a further constraint. This was provided by measurements performed by means of a blackbody box which enclosed the two antennas. Indicating with V_{cal} the radiometer output voltage when the antennas were covered with the blackbody box, and with T_{cal} the box physical temperature, the required solutions were derived from the following minimization formula:

$$\sum_{j=1}^{M}\left[(A+F\exp(-\tau m_j)-V_j)\right]^2+g[V_{cal}-B-GT_{cal}]^2=\min \qquad (14)$$

where g represents a weight to be attributed to the blackbody box measurements. As the value of g is increased the stability of the solutions improves consequently, but the solutions become necessarily biased towards that of the blackbody box measurement.

Figures 4 and 5 show the behaviour of B and G (τ behaves similarly to G) for a set of measurements during the campaign. For no constraint ($g=0$), large instabilities are evident thus making questionable a procedure based on the tipping curves only. However, it is noted that the bias B (figure 4) appears to become stable for small values of the weight g, while higher values of g are necessary to stabilize the solution for the gain G (figure 5) and the opacity τ. Therefore, the maximum value to

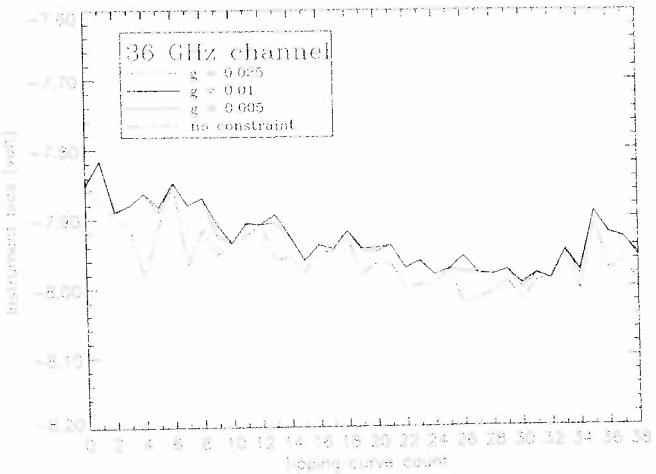

Figure 4. Radiometer bias at 36·0 GHz estimated from each of several tipping curve calibrations (tipping curve count on the horizontal axis) for different values of the weight g of the blackbody box constraint.

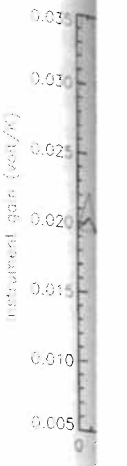

Figure 5. Radiometer
calibrations (tip
weight g of the

be given to g depend
Indeed, a warning sh
temperature sensors
uniformity of tempe
range of operations e
large and an evalua
performed before and
added a fixed amour
coupler and a variabl
applied to the blackb
the 20·6 GHz channel

Therefore, the bes
T_{cal} including in it th
simulation analysis sl
cent the error in the g
limitation of g to sm
particularly for the g
instrument stability a
computed an average
0·0203 V K^{-1} at 20·6
with laboratory tests
those computed for
continuous updating
measurement, has bee

5. Algorithm for esti

As far as the tota
been shown that ΔH c

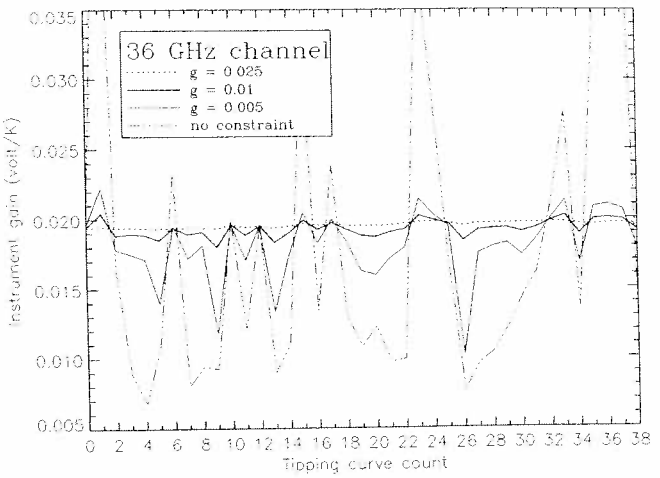

Figure 5. Radiometer gain at 36·0 GHz estimated from each of several tipping curve calibrations (tipping curve count on the horizontal axis) for different values of the weight g of the blackbody box constraint.

be given to g depends on how much we trust the blackbody box measurements. Indeed, a warning should be given on the accuracy of such measurements. Several temperature sensors have been used to estimate T_{cal}, but it is hazardous to assume uniformity of temperature through all the absorbing material. Furthermore, the range of operations corresponding to blackbody box and atmospheric radiations is large and an evaluation of the instrument linearity was necessary. This was performed before and after the experimental campaign by using a noise source which added a fixed amount of noise to the antenna temperature through a directional coupler and a variable attenuator. This allowed us to determine the correction to be applied to the blackbody physical temperature, that resulted in about 18 per cent for the 20·6 GHz channel and 15 per cent for the 36·0 GHz channel.

Therefore, the best choice of g depends on the accuracy assumed for the value of T_{cal} including in it the effectiveness of the instrument non-linearity correction. A simulation analysis showed that a value of g less than 0·01 limited to about 1 per cent the error in the gain, for an error in T_{cal} not larger than about 10 K. However, a limitation of g to smaller values still gave place to a certain degree of instability, particularly for the gain G and the opacity τ. Therefore, trusting in a reasonable instrument stability at least for the gain G while operating in AGC mode, we have computed an average value of G for $g=0{\cdot}01$. The obtained values of G equal to 0·0203 $V K^{-1}$ at 20·6 GHz and 0·0191 $V K^{-1}$ at 36·0 GHz appeared in agreement with laboratory tests and produced brightness temperatures that compared well with those computed for the RAOBs launched from the tower. On the contrary a continuous updating of the bias B, computed from the closest tipping curve measurement, has been used to calibrate each radiometer acquisition and estimate τ.

5. Algorithm for estimating the integrated atmospheric parameters

As far as the total (dry plus wet) excess path length is concerned, in § 2 it has been shown that ΔH can be expressed as a linear combination of the opacities at the

two frequencies and the atmospheric pressure. Moreover, to account for the minor influence of other parameters, the available meteorological data at the surface, such as temperature T_s and relative humidity RH_s, have been included as a linear constraint to the regression formula, so that we assumed:

$$\Delta H = a_0 + a_1\tau(f_1) + a_2\tau(f_2) + a_3 P_s + a_4 T_s + a_5 RH_s \tag{15}$$

In the absence of a suitable dataset including both radiometric and meteorological observations, the retrieval coefficients $a_0, a_1, \ldots a_5$ have been determined by using a large set of historical observations of the atmosphere obtained by available radiosoundings (RAOBs). Moreover, a radiative model has been used to simulate the values of brightness temperatures from the RAOBs data (Liebe 1989). The unknown retrieval coefficients were estimated by minimizing the sum of squares of the differences between the values of ΔH, calculated from the refractivity obtained from RAOBs (refractive ΔH), and the values predicted by (15), when simulated values of τ from the same RAOBs are used (radiative ΔH) (Basili *et al.* 1989). The effect of cloud liquid has been considered through a cloud model both for determining the refractive ΔH_1 and the simulated T_B (Decker *et al.* 1978). A similar regression analysis based on (15) can also be applied to predict the precipitable water vapour V and the integrated cloud liquid L.

Errors associated to each measurement have been considered by adding a Gaussian distributed random variable with a given r.m.s. The r.m.s. errors of the regressor variables P_s, T_s and RH_s were respectively 1 mbar, 0·2 K and 2 per cent, while those in the regressor variables τ derive by means of (9) from considering an r.m.s. fluctuation of T_{mr} and T_B of respectively 3·5 K and 1 K (conservative assumption considering possible imperfect calibration).

In the absence of sufficient meteorological data nearby the tower, use has been made of RAOBs data from the meteorological station of Udine only, besides those acquired at the tower. Being the Udine station at 94 m of altitude above the sea level, each profile has been supplemented with the data provided by the meteorological station of Venice (at sea level). More than four years of RAOB data have been processed and a stratification of the data has also been made according to the season and to clear and cloudy atmospheric conditions.

By stratifying data according to the season, we have only found a slight improvement on the accuracy of ΔH. On the contrary, the stratification based on meteorological conditions allowed us to achieve an appreciable improvement of r.m.s. error for clear sky reaching a value of 0·69 cm and no improvement for cloudy conditions with respect to non-stratified data, whose r.m.s. amounts to 0·82 cm. Figure 6 shows an example of the scatterplot of refractive values of ΔH against the ones obtained by regression for the summer season, consisting in a total of more than 2000 data points. We have also compared the refractive ΔH to the one computed by the Saastamoinen model (5) and (6), for the same set of the RAOBs data. In this case, the r.m.s. error becomes 2·4 cm and, therefore, we can assume that the radiometric measurements contributed to the reduction of such an error for about an 80 per cent.

As far as the regression analyses for the precipitable water vapour V and the integrated cloud liquid L are concerned, the residual r.m.s. errors were respectively 0·1 cm and 0·04 mm, starting from data bases having an average value of 3·0 cm for V and 0·2 mm for L.

6. Results

After having averaged
the excess path length
radiometer measurement
coefficients for clear sky
by the experimenter ope
directly derived from b
computed from the surfa
explained in § 5. A simila
and L.

The downward T_B a
radiometric measurement
available during the radi
time interval as close as
balloon data acquisition
of 6 hours between RAO
comparison. Indications
data have been already

Figures 7 and 8 sh
Although the points are
channel and 3·7 K for 3
(2·1 and 0·8 K for 20·6 a
ings launched from the
considered fairly success

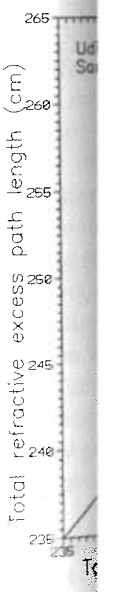

Figure 6. Scatterplot of t
from Udine summe
length predicted by
radiative ΔH). ΔH

6. Results

After having averaged the recording data stream and calibrated the instrument, the excess path length was computed straightforwardly by applying (15) to the radiometer measurements (radiometric ΔH). The selection of the correct set of coefficients for clear sky or cloudy conditions was based on the information supplied by the experimenter operating on the tower. The atmospheric opacity has been directly derived from brightness temperature T_B, using (9) and a value of T_{mr} computed from the surface meteorological data through a linear model as already explained in § 5. A similar linear regression procedure has been applied to estimate V and L.

The downward T_B and the three quantities ΔH, V and L estimated from the radiometric measurements have been compared to those obtained from RAOBs data available during the radiometer operation. The radiometric signal was averaged on a time interval as close as possible to each available radiosounding, considering that a balloon data acquisition can continue for about 2 hours. A maximum time interval of 6 hours between RAOBs and radiometer acquisitions has been considered in the comparison. Indications on the geographical distance between the two sources of data have been already reported in § 3.

Figures 7 and 8 show the comparison in terms of brightness temperature. Although the points are quite scattered (r.m.s. difference of 5·2 K for the 20·6 GHz channel and 3·7 K for 36·0 GHz), they do not show a significant biased behaviour (2·1 and 0·8 K for 20·6 and 36·0 GHz, respectively). Moreover, the two radiosoundings launched from the platform seem to indicate that the calibration can be considered fairly successful being the mean error of 1 K for the 20·6 GHz channel

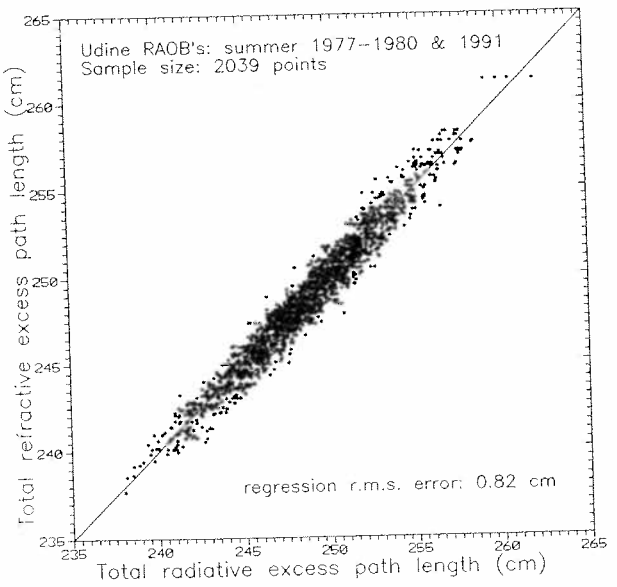

Figure 6. Scatterplot of the total excess path length calculated from the refractivity obtained from Udine summer season RAOBs (total refractive ΔH) versus the total excess path length predicted by the simulated τ from the same RAOBs through equation (15) (total radiative ΔH). ΔH is evaluated at the ERS-1 radar altimeter frequency of 13·8 GHz.

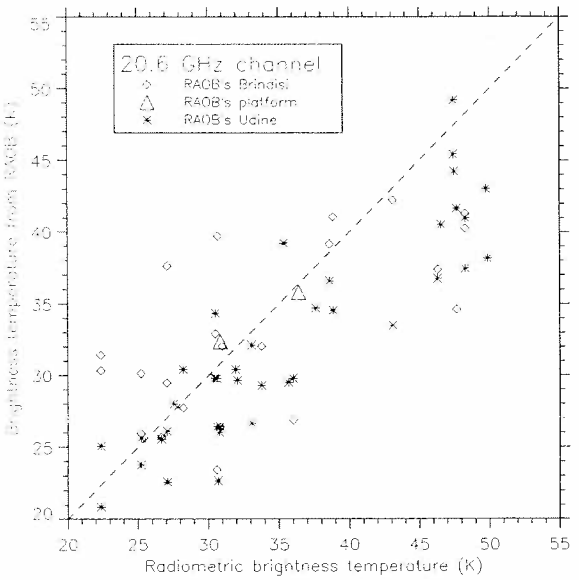

Figure 7. Brightness temperature T_B at 36·0 GHz computed from RAOBs versus radiometric T_B averaged on a time interval as close as possible to the corresponding RAOB. Brindisi, Udine and platform RAOBs are indicated by different symbols.

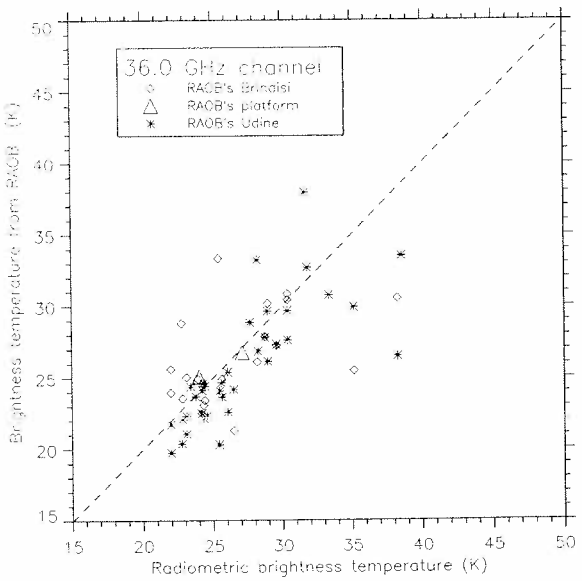

Figure 8. Brightness temperature T_B at 36·0 GHz computed from RAOBs versus radiometric T_B averaged on a time interval as close as possible to the corresponding RAOB. Brindisi, Udine and platform RAOBs are indicated bydifferent symbols.

Figure 9. Total e
meteorologi
time interva
ΔH). ΔH is
Udine and p
symbols.

and 0·7 K for th
assumed in the r
launched from t
instrument calibr

In figure 9, t
meteorological p
radiosoundings.
value of 1·5 cm a
is shown by the
from surface dat
ΔH. The compar
and a bias of −

As far as the
in figure 10. A fa
platform while th
of 0·2 cm.

In figure 11 v
T_B at 20·6 GHz
vapour V and in
worth noting th
liquid and the 3
microwave radio

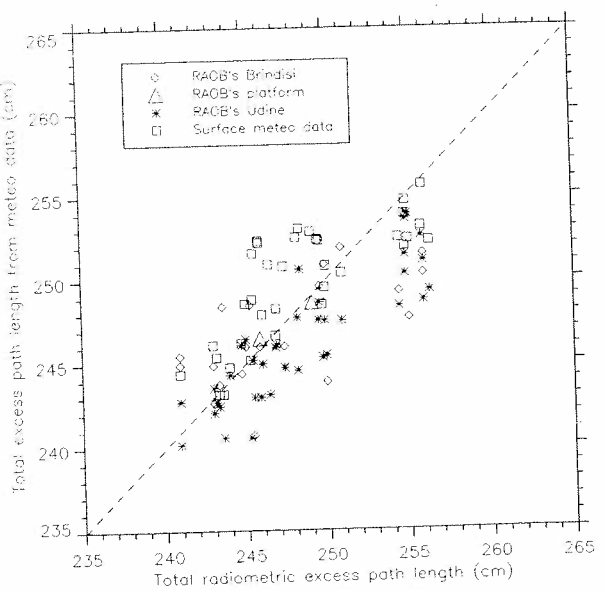

Figure 9. Total excess path length ΔH computed from meteo data (RAOBs or surface meteorological data) versus ΔH estimated from radiometric measurements avered on a time interval as close as possible to the corresponding meteo data (total radiometric ΔH). ΔH is evaluated at the ERS-1 radar altimeter frenquency of 13·8 GHz. Brindisi, Udine and platform RAOBs and surface meteorological data are indicated by different symbols.

and 0·7 K for the 36·0 GHz channel, which are within the error which has been assumed in the regression analysis. However, it appears that RAOBs that are not launched from the radiometer installation site cannot be used for validating the instrument calibration procedure.

In figure 9, the radiometric ΔH is compared to that estimated from surface meteorological parameters as in (5) and (6) and to refractive ΔH computed from radiosoundings. The difference between radiometric and refractive ΔH has a mean value of 1·5 cm and a standard deviation of 2·9 cm; however, a fairly good agreement is shown by the two radiosoundings released from the platform. ΔH estimations from surface data show a better agreement with the radiometer for small values of ΔH. The comparison with radiometric estimates shows a r.m.s. difference of 2·6 cm and a bias of $-1{\cdot}5$ cm.

As far as the precipitable water vapour V is concerned, the comparison is shown in figure 10. A fairly good agreement can again be noted for the two RAOBs at the platform while the overall comparison shows a r.m.s. difference of 0·5 cm and a bias of 0·2 cm.

In figure 11 we finally show an example of a temporal sequence of the measured T_B at 20·6 GHz and 36·0 GHz and of the derived estimates of precipitable water vapour V and integrated cloud liquid L for a single event of cloudy condition. It is worth noting the high correlation between the estimation of the integrated cloud liquid and the 36·0 GHz measured T_B, thus putting in evidence the capability of a microwave radiometer to infer the parameter L, not measurable by RAOBs.

7. Conclusions

The work presented in this paper was mainly devoted to the estimation of the tropospheric correction of the ERS-1 radar altimeter by using measurements provided by a dual-channel microwave radiometer installed on an oceanographic tower.

The procedure for retrieving the excess path length together with other integrated atmospheric parameters was based on a historical set of meteorological data that allowed us to produce, by using a radiative model, a large database of both atmospheric parameters and simulated brightness temperatures. The method allowed a fine adaptation to the climatological conditions of the geographical area leading to a r.m.s. accuracy of about 0·8 cm in ΔH, 0·1 cm in V and 0·04 mm in L, without considering radiometric calibration errors.

The problem of calibration was approached by using measurements feasible in a site where adequate laboratory equipment were not available. A procedure, based on tipping curve calibrations and a blackbody box at ambient temperature, was successfully adopted to monitor both instrument gain and bias. A good agreement (within a maximum error of 1 K) was found between the radiometric downward radiation measurements and the brightness temperatures computed from radiosoundings launched from the same site.

The validation of the retrieved atmospheric parameters using data collected in the Meteorological Service RAOB Stations was not reliable because of the distance from the experiment location which brought out the effects of the non-homogeneity of the atmosphere. However, the results obtained from the few radiosoundings launched at the tower agreed very well with those derived from the radiometer measurements, within the r.m.s. error of the retrieval algorithm.

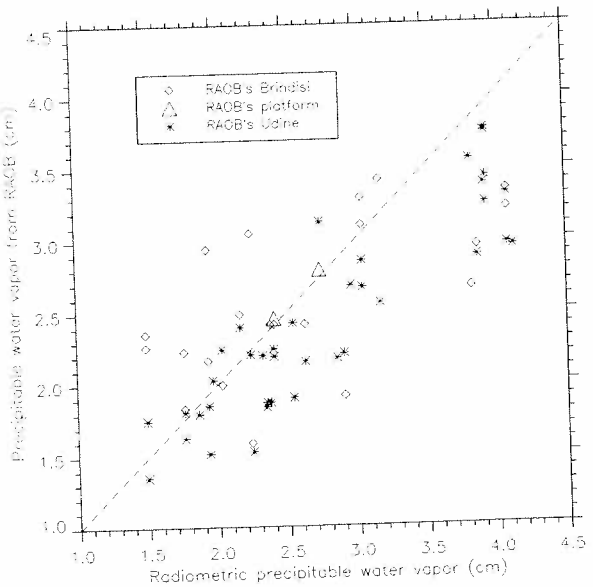

Figure 10. Precipitable water vapour V computed from RAOBs versus V estimated from radiometric measurements averaged on a time interval as close as possible to the corresponding RAOB (radiometric V). Brindisi, Udine and platform RAOBs are indicated by different symbols.

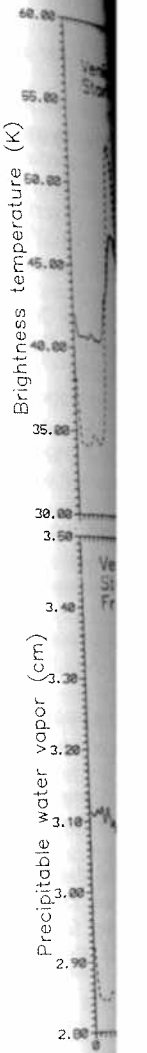

Figure 11. Tempor
36·0 GHz (to
integrated cl

Acknowledgments

The authors
Tor Vergata Un
Research Council
I.S.D.G.M.) for t
campaign, Mr M
Geofisico of the
(ITAV) for the m
Italian Ministry
Agency (ASI) an

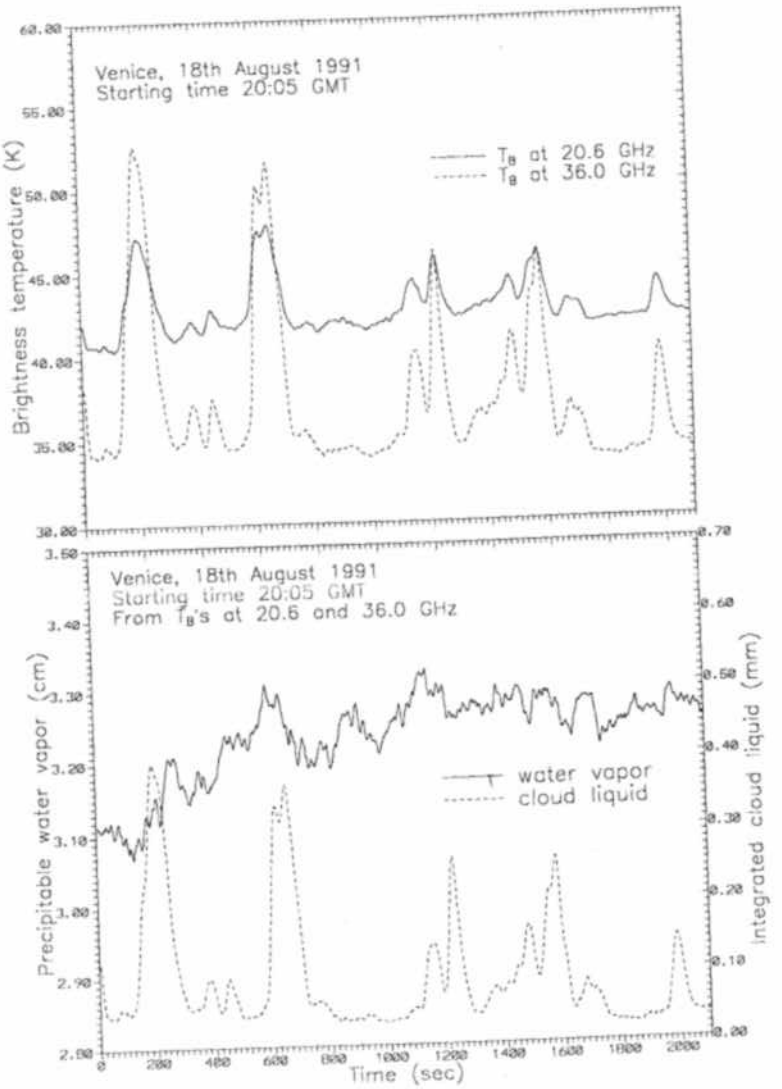

Figure 11. Temporal sequence of the measured brightness temperature T_B at 20·6 GHz and 36·0 GHz (top panel) and corresponding estimates of precipitable water vapour and integrated cloud liquid (bottom panel) during a cloudy event.

Acknowledgments

The authors would like to thank the Department of Ingegneria Elettronica of Tor Vergata University of Rome for providing the radiometer, the National Research Council/Istituto per lo Studio della Dinamica delle Grandi Masse (C.N.R./I.S.D.G.M.) for the facilities on the platform and for precious help during the whole campaign, Mr Moreno De Angelis for operating the radiometer, the Osservatorio Geofisico of the University of Modena and the Italian Meteorological Service (ITAV) for the meteorological data. The work has been partially supported by the Italian Ministry of University and Scientific Research (MURST), the Italian Space Agency (ASI) and the European Space Agency (ESA).

References

BASILI, P., CIOTTI, P., and D'AURIA, G., 1989, Improving accuracy in radar-altimetry data correction for tropospheric effects. *Electronics Letters*, **25**, 458–459.

BASILI, P., CIOTTI, P., and FIONDA, E., 1994, Comparison of algorithms for retrieval of water vapour, cloud liquid and atmospheric attenuation by microwave radiometry. In *Proceedings of PIERS '94 Symposium, held in Noordwijk, The Netherlands on 11–15 July 1994* (Noordwijk, The Netherlands: Kluwer Academic Publishers), pp. 571–574.

BEAN, B. R., and DUTTON, E. J., 1968, *Radio Meteorology* (New York: Dover).

DECKER, M. T., WESTWATER, E. R., and GUIRAUD, F. O., 1978, Experimental evaluation of ground-based microwave radiometric sensing of atmospheric temperature and water vapor profiles. *Journal of Applied Meteorology*, **17**, 1788–1795.

DUCHOSSOIS, G., 1991, The ERS-1 Mission Objectives. *ESA Bulletin*, **65**, 16–26.

FRANCIS, C. R. (editor), 1993, The Calibration of the ERS-1 Radar Altimeter. Report ER-RP-ESA-RA-0257, Issue 2.0, ESA/ESTEC Noordwijk, The Netherlands.

GOLDFINGER, A. D., 1980, Refraction of microwave signals by water vapor. *Journal of Geophysical Research*, **85**, 4904–4912.

GOLDHIRSCH, J., and ROWLAND, J. R., 1982, A tutorial assessment of atmospheric height uncertainties for high-precision satellite altimeter missions to monitor ocean currents. *I.E.E.E. Transactions on Geoscience and Remote Sensing*, **20**, 418–434.

LIEBE, H. J., 1989, MPM'89—An atmospheric millimeter wave propagation model. *International Journal IR & MMWaves*, **10**, 631–650.

RESCH, G. M., 1984, Water vapor radiometry in geodetical applications. In *Geodetic Refraction*, edited by F. K. Brunner (Berlin: Springer-Verlag).

SAASTAMOINEN, J., 1972, Atmospheric correction for the troposphere and stratosphere in radio ranging of satellites. In *Geophysical Monography 15*, edited by A.G.U. (Richmond (VA): William Byrd).

SLOBIN, S. D., 1982, Microwave noise temperature and attenuation of clouds: statistics of these effects at various sites in the U.S., Alaska and Hawaii. *Radio Science*, **17**, 1443–1454.

ULABY, F. T., MOORE, R. K., and FUNG, A. K., 1981, *Microwave Remote Sensing: Active and Passive. Volume I: Microwave Remote Sensing Fundamental and Radiometry* (London: Addison-Wesley).

WESTWATER, E. R., 1978, The accuracy of water vapor and cloud liquid determination by dual-frequency ground-based microwave radiometry. *Radio Science*, **13**, 677–685.

WU, S. C., 1979, Optimum frequencies of a passive microwave radiometer for tropospheric path-length correction. *I.E.E.E. Transaction on Antennas and Propagation*, **27**, 233–239.